

FILE COPY

 National Defence / Défense nationale

UNCLASSIFIED

2

UNLIMITED DISTRIBUTION

**DRES**

**SUFFIELD MEMORANDUM**

AD-A209 084

NO. 1264

**INFRARED REFLECTANCE  
MEASUREMENTS OF REPLICA MINES  
AND  
REFERENCE TARGETS (U)**

by

**DISTRIBUTION STATEMENT A**  
Approved for public release;  
Distribution Unlimited

G.C. Stuart  
Ordnance Detection Group

**SDTICD**  
ELECTE  
JUN 16 1989  
H

February 1989



**DEFENCE RESEARCH ESTABLISHMENT SUFFIELD, RALSTON, ALBERTA**

**WARNING**  
The use of this information is permitted subject to recognition of proprietary and patent rights.

Canada

89 6 16 317

UNCLASSIFIED

Infrared Reflectance Measurements of Replica  
Mines and Reference Targets(U)

G. C. Stuart  
Ordnance Detection Group

**SUFFIELD MEMORANDUM NO. 1264**  
Defence Research Establishment Suffield  
Ralston, Alberta  
TOJ 2N0

**WARNING**  
"The use of this information is permitted subject to  
recognition of proprietary and patent rights".

UNCLASSIFIED

UNCLASSIFIED

Executive Summary

Remote minefield detection (RMD) can be performed by mounting downward-looking sensors on airborne platforms such as remotely-piloted vehicles (RPVs). Scatterable mines lying on the surface of the ground may be detected using a carbon-dioxide laser mounted on the RPV as a source of thermal infrared radiation and by measuring the reflected signals to create an image of the terrain below. Such an active infrared system is capable of operating covertly at all times of the day or night and makes use of much of the technology found in current passive infrared sensors (ie. forward-looking infrared imagers, FLIRs, on military aircraft, ground vehicles, and ships).

This report presents reflectance data on a number of replica mines which have been found to be specular (mirror-like) at thermal IR wavelengths. The measurements of the replica mines and a number of reference materials were made in a laser laboratory, and retro-reflectivity data for each target are presented graphically as a function of the angle at which the IR laser beam hit the target surface. The fact that the replica mines are specular means that the RMD sensor must be downward-looking and only those mines within a fairly small angular field-of-view will give significantly large reflected signals.

*Replica mine interesting for detection*



Accession For	
NTIS GRA&I	<input checked="" type="checkbox"/>
DTIC TAB	<input type="checkbox"/>
Unannounced	<input type="checkbox"/>
Justification	
By	
Distribution/	
Availability Codes	
Dist	Avail and/or Special
A-1	

UNCLASSIFIED

UNCLASSIFIED

**Abstract**

The 10.6  $\mu\text{m}$  reflectance characteristics of a number of targets were measured to establish a preliminary database for studies in remote minefield detection (RMD) and to verify experimental techniques. The reflectivities of typical mine-casing materials and mine paints were found to be highly specular, although there was substantial variation in the magnitudes of the returns. The measured reflectances of diffuse reference targets were in reasonably good agreement with previously published data.

In addition to the numerical results, a qualitative study of reflectance using an infrared camera and CO<sub>2</sub> laser illumination proved useful in the rapid investigation of target reflectivity. The implications of the results of the study of mine materials to the feasibility of airborne RMD are discussed and suggestions are made for future in-depth experiments.

UNCLASSIFIED

# Contents

<b>1</b>	<b>Introduction</b>	<b>1</b>
<b>2</b>	<b>Targets</b>	<b>3</b>
2.1	Scatterable Mines . . . . .	3
2.2	Reference Targets . . . . .	8
<b>3</b>	<b>ODG Laser Laboratory and Equipment</b>	<b>11</b>
3.1	Lasers and Optics . . . . .	11
3.2	IR Detection and Monitoring . . . . .	12
3.3	IR Camera System . . . . .	13
<b>4</b>	<b>Experimental Arrangement</b>	<b>15</b>
4.1	Monitoring of CO <sub>2</sub> laser . . . . .	15
4.2	Calibration of the HgCdTe detectors . . . . .	17
4.3	Reflectance Study using the Infrared Camera . . . . .	17
4.4	Quantitative Reflectance Measurements . . . . .	18
<b>5</b>	<b>Results</b>	<b>23</b>
5.1	Qualitative Studies . . . . .	23
5.2	Quantitative Reflectance Data . . . . .	25
5.2.1	Replica Mines . . . . .	25
5.2.2	Reference Targets . . . . .	30
<b>6</b>	<b>Discussion</b>	<b>34</b>
6.1	Summary of Results . . . . .	34
6.2	Specular Mines and RMD . . . . .	34
6.3	Future Studies . . . . .	35
<b>7</b>	<b>References</b>	<b>37</b>
<b>A</b>	<b>Equipment Information</b>	<b>38</b>

## List of Tables

A.1 List of equipment used in IR reflectance studies . . . . . 39

## List of Figures

2.1	Replica TMN-46 mine . . . . .	4
2.2	Replica PMN-6 mine . . . . .	5
2.3	Replica OZM-3 mine . . . . .	6
2.4	Replica PFM-1 mine . . . . .	7
2.5	Imaging of diffuse surface . . . . .	9
3.1	IR camera system . . . . .	14
4.1	Arrangement to obtain and monitor CO <sub>2</sub> laser beam . . . . .	16
4.2	Arrangement for qualitative study of reflectance . . . . .	19
4.3	Arrangement for quantitative reflectance measurements . . . . .	20
4.4	Target areas on replica mines . . . . .	21
5.1	Active infrared image of replica PMN-6 mine . . . . .	24
5.2	Active infrared image of replica PFM-1 mine . . . . .	26
5.3	Reflectance curve for replica TMN-46 mine . . . . .	27
5.4	Reflectance curves for replica PMN-6 and OZM-3 mines . . . . .	28
5.5	Reflectance curve for replica PFM-1 mine . . . . .	29
5.6	Reflectance curve for "smooth" FSA plate . . . . .	31
5.7	Reflectance curve for "rough" FSA plate . . . . .	32
5.8	Reflectance curve for canvas . . . . .	33

# 1. Introduction

The Ordnance Detection Group (ODG) at Defence Research Establishment Suffield (DRES) is investigating the feasibility of remote minefield detection (RMD) using optical methods. Surface-laid mines may be distinguished from natural backgrounds using active thermal infrared (IR) methods, and high-resolution airborne CO<sub>2</sub> laser radars have been identified as promising sensors for the detection of scatterable minefields[1]. This document reports on the results of preliminary measurements of the 10.6  $\mu\text{m}$  reflectance of a limited number of objects and materials. A good understanding of the reflectance characteristics of materials is required for the design and operation of an active infrared RMD sensor. Accurate reflectivity data are also required for simulated active IR images which are being used in the development of image processing algorithms[2].

A complete description of the reflectance of an object is given by the bi-directional polarized reflectance distribution function (BPRDF). This function characterizes the reflectance in terms of the magnitude and polarization of the reflected radiation over all possible combinations of incidence and observation angles. For a given wavelength,  $\lambda$ , the BPRDF of a surface is  $\mathcal{F}(\lambda; \theta_i, \phi_i, \mathcal{P}_i; \theta_r, \phi_r, \mathcal{P}_r)$  where the subscripts  $i$  and  $r$  indicate the incident and reflected radiation.  $\theta$  is the polar angle measured from the normal to the surface and  $\phi$  is the azimuthal angle. The polarization state of the radiation is  $\mathcal{P}$ . However the geometry of the proposed RMD system [1] is such that only the target's retroreflectance is important. A downward-looking CO<sub>2</sub> laser radar, mounted on a remotely piloted vehicle (RPV), acquires high-resolution images of the terrain over which the vehicle is flying. The illumination and detection directions are equal ( $\theta_i = \theta_r, \phi_i = \phi_r$ ) in the case of this airborne monostatic laser radar.

The preliminary measurements reported in this document were of the magnitude of the retroreflectance from various targets as a function of the target aspect angle. The IR reflectivities of replica Soviet mines, which are made of typical mine materials and coatings, and those of standard CO<sub>2</sub> laser radar reference targets were studied. Quantitative reflectance data was obtained by arranging a CO<sub>2</sub> laser beam to be incident on the surface of a target and measuring the retroreflected signal power with a HgCdTe photoconductive detector. A rapid qualitative means of character-

izing the reflectance of complicated three-dimensional objects was developed using a commercial IR camera system and an expanded CO<sub>2</sub> beam.

The aim of this study was to get a better understanding of the infrared reflectance characteristics of a select number of targets and to develop and verify experimental techniques which will be used in future in-depth studies. The emphasis was to reveal and/or confirm some of the important aspects of the RMD problem with a view to determining limits for the design and operation of an airborne RMD CO<sub>2</sub> laser radar system. Mines and other man-made objects tend to be predominantly specular in the thermal infrared and the reflectances measured in this study confirmed this trend. However there were certain mine materials which were found to have far less specular reflectances than other materials. The results are discussed in terms of their impact on the RMD problem and the measured reflectances are compared with other published infrared data. Suggestions are made for further experimental study and for refinements to the reflectance measurement system.

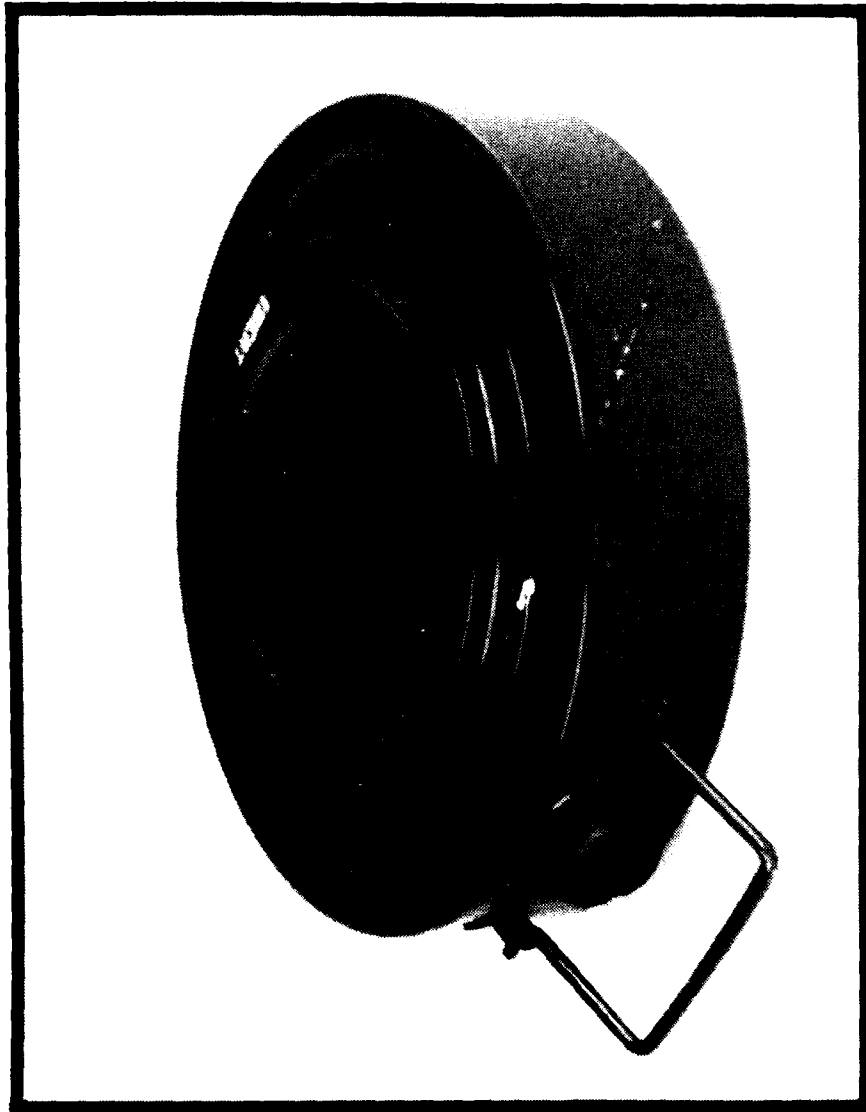
## 2. Targets

### 2.1 Scatterable Mines

The targets of interest in remote minefield detection are surface-laid scatterable mines. These mines have either plastic or metal cases and they vary considerably in size, although they tend to be smaller than other types of mines. Scatterable mines are frequently coated with standard military camouflage paints in order to make them less detectable at visible wavelengths. There can be significant variation in the shapes of scatterable mines but the majority, like their conventional counterparts, are cylindrical.

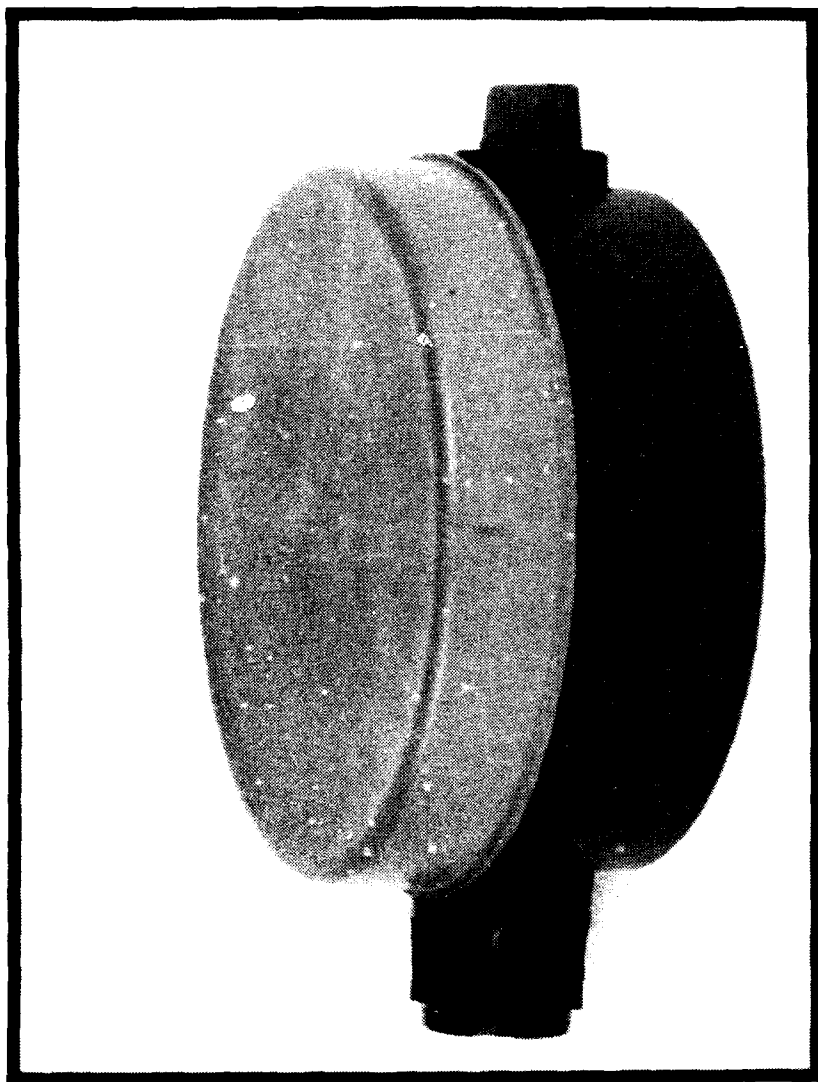
This report presents data on the reflectance of a number of replica Soviet mines. These full-sized mine replicas [3] were manufactured for training purposes and they use materials and paints which approximate those of the Soviet mines. The replica and actual mines are only similar in the visible portion of the electromagnetic spectrum and they may differ at other wavelengths. The 10.6  $\mu\text{m}$  reflectivities of four different models of Soviet mine were measured, and Figures 2.1 through 2.4 show photographs of the replica TMN-46, PMN-6, OZM-3, and PFM-1 mines used in this study. Note that the mines are designated using their Soviet model numbers.

The PFM-1 is a small aircraft-delivered anti-personnel mine which is commonly known as the "butterfly" mine for obvious reasons. The body of the PFM-1 used in these reflectance experiments is made of green polystyrene. The wingspan of the butterfly mine is 12 cm. Both the OZM-3 and PMN-6 are also anti-personnel mines, with the latter having the potential to be deployed from trucks. The OZM-3 is a green-painted steel cylinder 12 cm high with a diameter of 7.5 cm. The 12 cm diameter top cover of the PMN-6 is made of soft green rubber while the rest of its body is a brown thermoplastic. The TMN-46 is a large conventional anti-tank mine with a diameter of 31 cm. This mine would usually be buried in combat however its olive-drab painted metal casing is characteristic of artillery and air-delivered scatterable anti-tank mines. The Soviets are actively developing these forms of scatterable mines which will be similar to the U.S. M-70 RAAM (Remote Anti-Armor Mine).



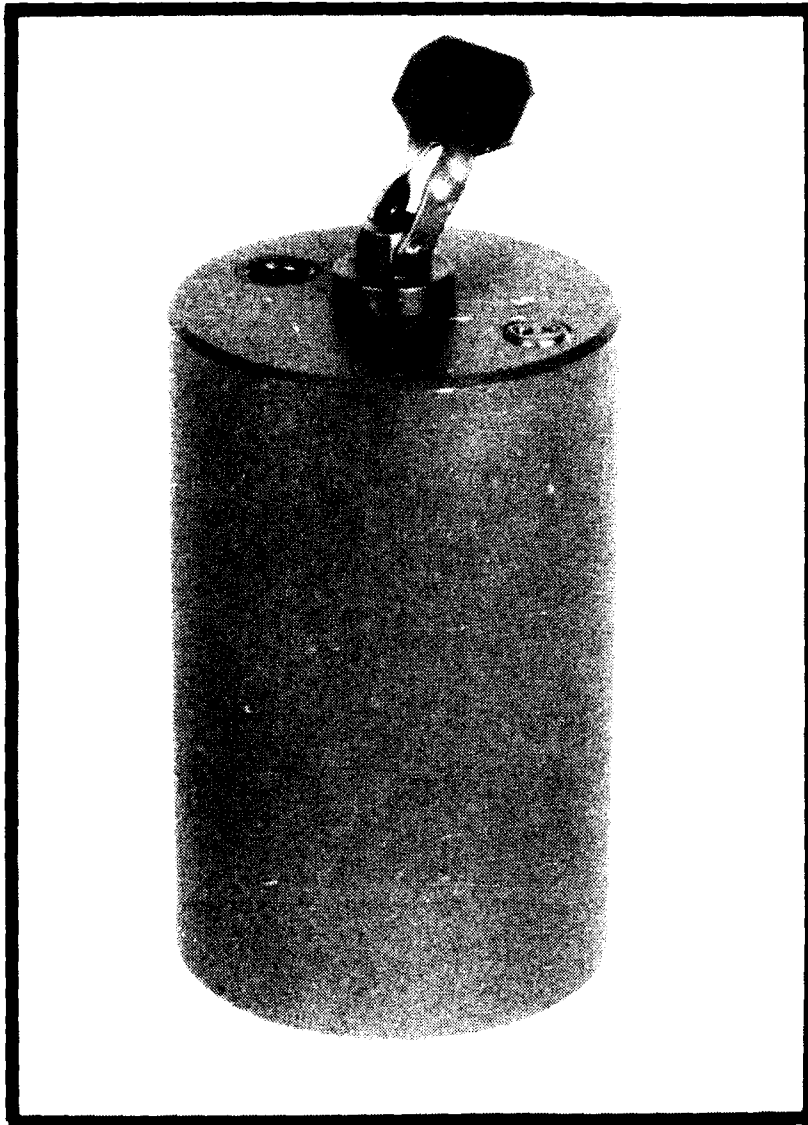
88-335

Figure 2.1  
REPLICA TMN-46 MINE



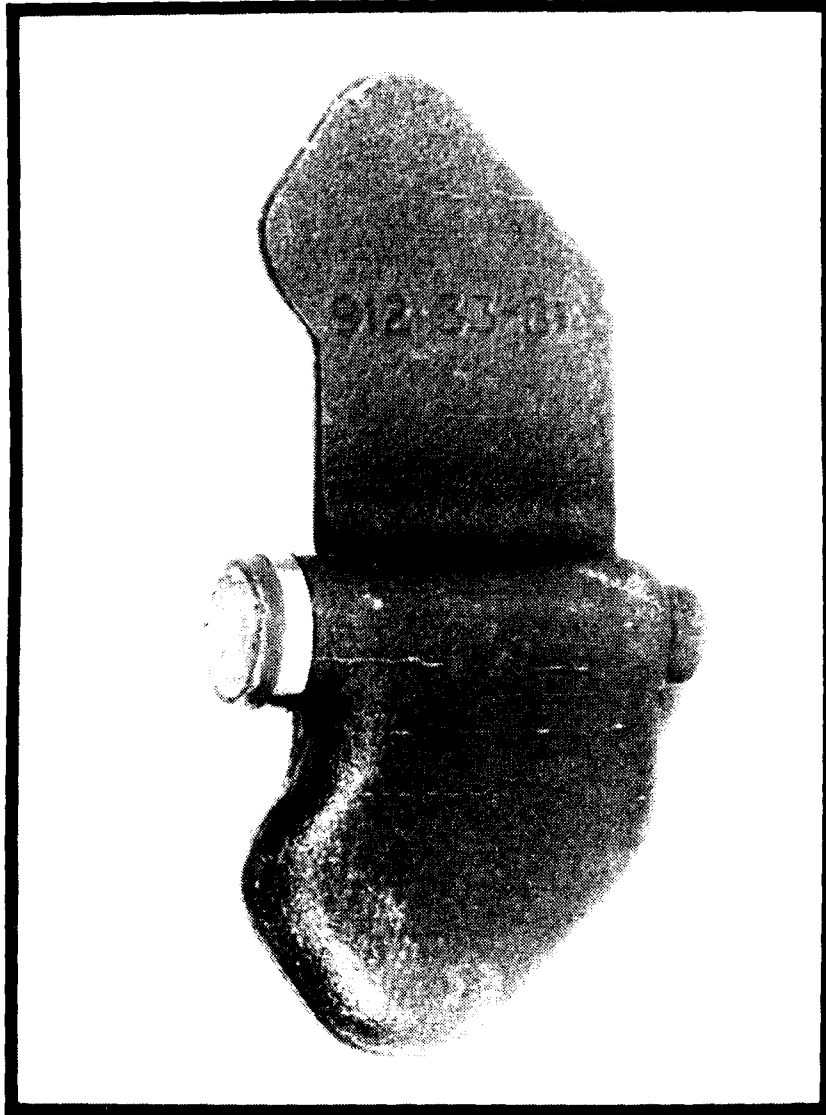
88-335

Figure 2.2  
REPLICA PMN-6 MINE



88-335

Figure 2.3  
REPLICA OZM-3 MINE



BB-335

Figure 2.4  
REPLICA PFM-1 MINE

## 2.2 Reference Targets

In addition to the replica mines a number of other targets were studied, both for the purposes of calibration of the measurement system and for verifying their future suitability as reference targets. A reference target for a CO<sub>2</sub> laser radar should have well-defined reflectance characteristics and be useful over as wide a range of incident angles as possible. Consequently standard reference targets for laser radars are most often diffuse and have reflectances which are close to those of Lambertian surfaces. The radiance of such a Lambertian surface is  $L = \rho P_i / \pi$  where  $\rho$  is the hemispherical reflectance (albedo) and  $P_i$  is the incident laser power. The scattered intensity, measured in terms of power per steradian, is proportional to the cosine of the viewing angle,  $\theta$ , and is given by  $I = L \cos \theta$ . The diffuse reflectivity,  $R_{diff}(\theta)$ , is a commonly used parameter which is defined as,  $R_{diff}(\theta) = \rho \cos \theta$ , and represents the ratio of the scattered signal to that which would be measured from an ideal, 100 % reflecting Lambertian surface with  $\theta = 0^\circ$ .

Consider the situation shown in Figure 2.5 where a lens is being used to image a diffuse surface onto a detector. The lens, which has an area,  $A_{lens}$ , is a distance  $l$  from the surface and the detector, with an area  $A_d$ , is at the focus of the lens. The solid angle field-of-view (FOV) of the detector is

$$\Omega_{fov} = \frac{A_d}{f^2} = \frac{A_s}{l^2}$$

where  $A_s$  is the area subtended on the diffuse surface. If  $L$  is the radiance of the surface then the power received by the detector is

$$P_d = \frac{L A_s A_{lens}}{l^2} = L \Omega_{fov} A_{lens}.$$

The diffuse reflectivity can be determined using the known geometry and the measured values of  $P_i$  and  $P_d$ :

$$R_{diff}(\theta) = \frac{\pi}{A_{lens}} \frac{P_d}{\Omega_{fov} P_i}.$$

The diffuse targets used in these experiments were flame-sprayed aluminum and a military tent canvas. These targets are preferable to other possible materials commonly used as standard 10.6  $\mu\text{m}$  references, such as slurried salt or sublimed sulfur, because they are durable, easy to work with, and can readily be used in the field.

UNCLASSIFIED

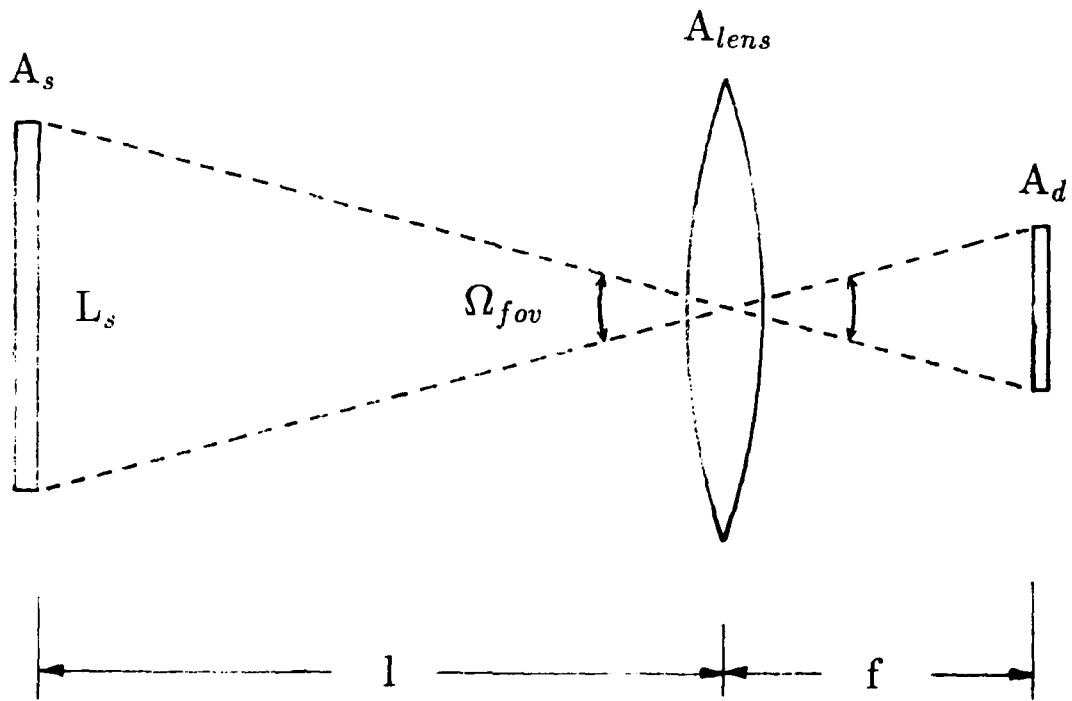


Figure 2.3: Imaging of diffuse surface

UNCLASSIFIED

Flame-sprayed aluminum (FSA) has been one of the most widely used CO<sub>2</sub> laser radar target materials. There can be substantial variability in the reflectances of FSA plates due to differences in the methods of preparation. The IR reflectance of two samples of flame-sprayed aluminum were measured in this study. The origins of one of the FSA plates was unknown, while the second FSA plate was prepared as follows:

20-grit sifted chilled iron was "sandblasted" onto a 3.2 mm thick aluminum plate to roughen the surface. The plate was then sprayed with nickel aluminide base-bond agent (METCO 405) followed by pure aluminum. The total thickness of the sprayed coating was found to vary between 0.38 and 0.51 mm.

This method of preparation is similar to that described in [4] and [5]. The resulting FSA plate had a far rougher surface than that of the other sample. Consequently throughout this report the two flame-sprayed aluminum samples will be referred to as the "rough" and "smooth" FSA plates.

Canvas has recently been proposed as a suitable CO<sub>2</sub> laser radar reference target material [6]. A canvas sample was obtained from Defence Research Establishment Valcartier (DREV) and its 10.6  $\mu\text{m}$  reflectance measured. The canvas was a military tent canvas made with 10 oz. treated material and with a mineral linen color.

### 3. ODG Laser Laboratory and Equipment

The Ordnance Detection Group laser laboratory was developed to conduct optical experiments in support of the RMD program, specifically the studies at thermal infrared wavelengths. Since it is a new facility at DRES, a general description of the laboratory and of the equipment within it is in order. The experimental arrangements used for both the qualitative and quantitative IR reflectance measurements are described in detail in Section 4. Appendix A gives information on the manufacturers and model numbers of the various pieces of equipment used in the infrared experiments.

The IR reflectance studies were performed on a 3.05 m long by 1.22 m wide vibration-isolated optical table which was located in a light-tight interlocked room. The isolators for the table, operating as air-springs, were supplied with compressed zero-grade air at a pressure of 38 psi. The stainless-steel top skin of the optical table had tapped  $\frac{1}{4}$ -20 NC holes on 2.54 cm centers for the mounting of optical equipment.

#### 3.1 Lasers and Optics

The source of the 10.6  $\mu\text{m}$  infrared radiation was a stabilized, grating-tuned, continuous-wave  $\text{CO}_2$  laser. This Class IV laser was tunable through both the 9.4  $\mu\text{m}$  and 10.4  $\mu\text{m}$  wavelength bands and could operate on any one of a possible eighty laser transitions. The 80 cm long discharge drew a current of 6.3 mA at a voltage of 20 kV. The laser power supply was tripped if the interlock switches at the access points to the room were opened. The nominal power of the horizontally-polarized  $\text{TEM}_{00}$  output beam of the  $\text{CO}_2$  laser was 10 W. The initial beam cross-section at the output coupler was elliptical, with a horizontal size of 3.0 mm and a vertical size of 3.7 mm. The horizontal full-angle divergence of 4.5 mrad and the vertical divergence of 3.6 mrad resulted in a far-field elliptical spot with the major axis in the horizontal plane. The output intensity of the  $\text{CO}_2$  laser beam was 115  $\text{W}/\text{cm}^2$ . The laser used a closed-cycle distilled water cooling system to maintain the discharge temperature

at 20° C. The output power of the CO<sub>2</sub> laser could be stabilized to  $\pm 0.5\%$  using a dither stabilization unit. This unit controlled the movement of the laser's output coupler which was mounted on an electro-mechanical mirror translator (EMT). An oscilloscope was used to monitor the operation of the CO<sub>2</sub> laser stabilization unit.

A number of small 0.5 mW helium-neon (HeNe) lasers were used for the alignment of optical components. The visible red (632.8 nm) HeNe beams were introduced so as to make them coaxial with the infrared CO<sub>2</sub> beams. Marking the IR beams with the visible HeNe beams also provided an additional level of safety during the experiments. CO<sub>2</sub> laser safety goggles were mandatory for all personnel in the laboratory during operation of the CO<sub>2</sub> laser.

Germanium (Ge) and zinc selenide (ZnSe) were used as transmissive optical materials in the infrared, while front-surfaced aluminum (Al) mirrors served as reflective optics. These aluminum mirrors had protective coatings of silicon oxide and reflectivities of 97 % in the thermal infrared. At 10  $\mu\text{m}$  the refractive index of germanium is 4.0 and zinc selenide has a refractive index of 2.4. Most of the transmissive IR optics were therefore anti-reflection coated. ZnSe had a distinct advantage over Ge in that it was translucent to the HeNe radiation.

### 3.2 IR Detection and Monitoring

A CO<sub>2</sub> laser spectrum analyzer was used to monitor the wavelength of the infrared radiation, and thermal image plates were used for IR beam alignment and diagnosis. The display screen of the spectrum analyzer and the screens of the image plates utilized the principle of thermally-inhibited fluorescence. Light from ultraviolet lamps caused the thermo-sensitive phosphors of the thermal plate screens to fluoresce and thus reveal the intensity profile of the CO<sub>2</sub> laser beams. A selection of thermal image plates covered a range of IR beam intensities from 60 mW/cm<sup>2</sup> to 200 W/cm<sup>2</sup>. Heat-sensitive liquid-crystal sheets were also used for infrared detection and beam alignment.

The output power of the CO<sub>2</sub> laser and other large IR signals were measured with a surface-absorbing disc calorimeter. This laser power meter was rated for a maximum input power density of 200 W/cm<sup>2</sup> and had an accuracy of  $\pm 3\%$ . The smaller IR signals reflected from the target surfaces during the quantitative measurements were detected using one of two available photoconductive (PC) infrared detectors. These mercury-cadmium-telluride (HgCdTe) detectors were liquid-nitrogen (LN<sub>2</sub>) cooled to 77 K and their spectral responses peaked at 10  $\mu\text{m}$ . One HgCdTe detector had an active area of 4.1 mm<sup>2</sup> while the other detector had a 1 mm<sup>2</sup> active area. The detector elements were housed in dewars with 60° fields-of-view (FOV), and were matched to preamplifier units. Bias currents to the detectors were provided using a regulated dc

power supply.

The HgCdTe detectors were AC-coupled and required time-varying infrared signals. The reflectance measurements were therefore made with a chopped CO<sub>2</sub> laser beam which was obtained by passing the output of the CO<sub>2</sub> laser through a rotating-disk light-beam chopper. The resultant chopped infrared beam had a 50 % duty cycle and the chopper control unit provided a 5 V square-wave reference signal. The signals from the HgCdTe detectors were displayed on an oscilloscope along with the chopper reference signal, which also provided the trigger for the scope. The rms value of the signal from the HgCdTe detector measuring the reflected radiation from the target was displayed on a digital voltmeter.

### **3.3 IR Camera System**

An infrared camera system was used for the rapid qualitative assessment of target reflectance. The system, shown in Figure 3.1, was based around an Thermovision-782 IR camera. The scanner used a LN<sub>2</sub>-cooled PC HgCdTe single-element detector, germanium optics coated for 10 μm, and image-space scanning to generate a 100 by 70 pixel thermal infrared image. Two different Ge input lenses were used with the IR scanner. A 20° × 20° field-of-view lens provided a spatial resolution of 3.5 mrad while the resolution of a 3.5° × 3.5° FOV lens was 0.6 mrad. Extension rings were used with the 3.5° lens to reduce the minimum focal distance to just over 1 m and give a scanned field of the order of 5 cm wide. Most of the qualitative reflectance study was made using the 20° lens which had a field approximately 15 cm wide at the minimum focus of 50 cm. A filter, with a 0.25 μm bandpass centered at 10.6 μm, was used to limit the detected radiation to CO<sub>2</sub> laser wavelengths.

The non-standard composite B/W video output of the Thermovision IR camera was converted into NTSC video by a scan converter. With the converter in its frame-hold mode the video frames, corresponding to the 10.6 μm images of the CO<sub>2</sub> laser-illuminated targets, were digitized at a resolution of 320 × 200 using a hardware/software package and a personal computer. A video monitor displayed each frame as it was being digitized. The infrared images were stored in IFF (Interchange File Format) and hardcopy was obtained via a laser printer. When the scan converter was operating in real-time the monitor provided a convenient alternative to the small screen of the Thermovision control and display unit. Photographs of this display were also used to record the infrared images.

UNCLASSIFIED

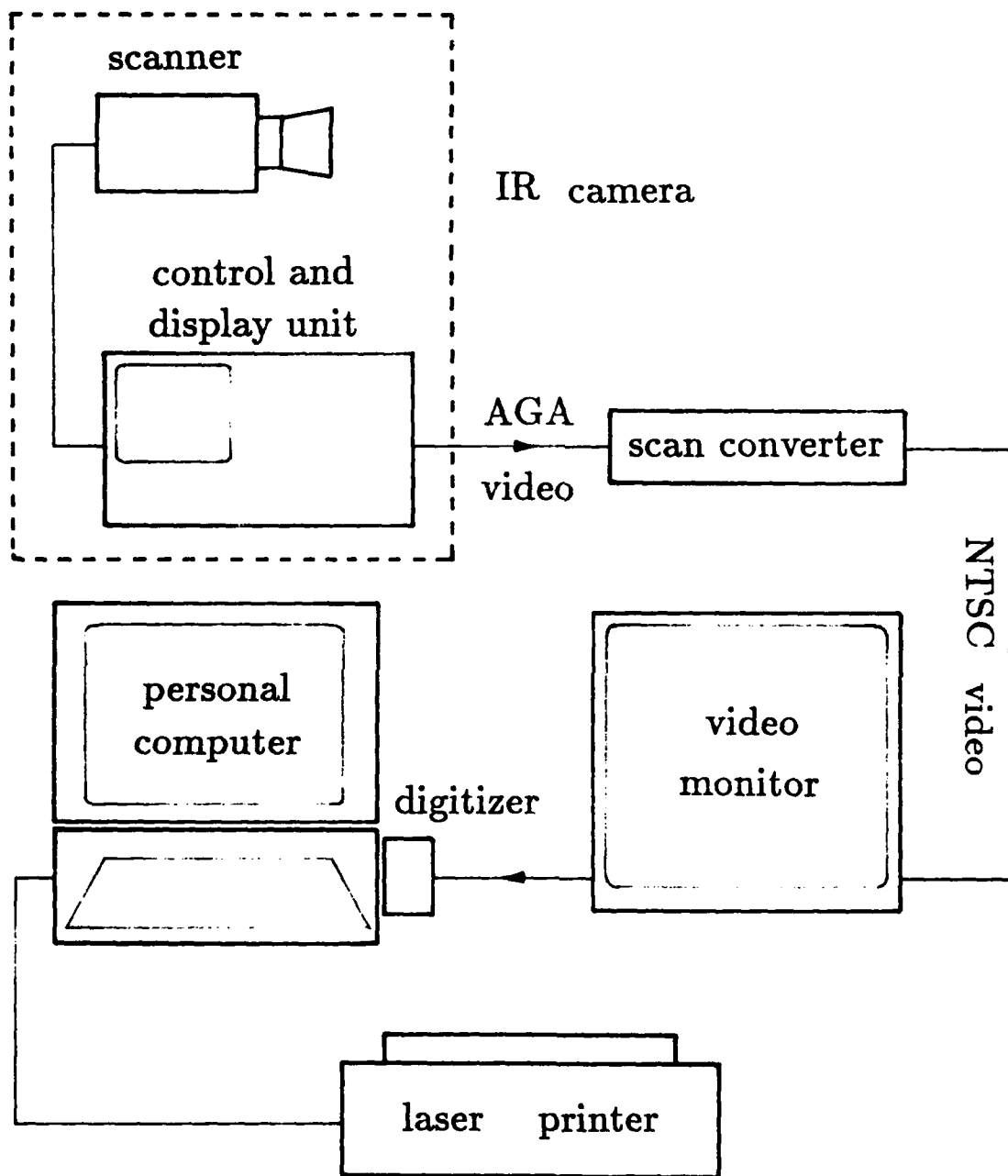


Figure 3.1: IR camera system

UNCLASSIFIED

## 4. Experimental Arrangement

### 4.1 Monitoring of CO<sub>2</sub> laser

The basic arrangement of Figure 4.1 was common to all of the infrared reflectance experiments reported here. The figure shows how the output of the CO<sub>2</sub> laser was monitored, chopped, and marked with visible HeNe beams. All the optical components were 50.8 mm in diameter and were mounted in either commercial or custom-built mounts. Note that unless otherwise specified all the mirrors shown in this and subsequent diagrams were flat front-surfaced aluminum mirrors.

The initial CO<sub>2</sub> laser beam passed through an uncoated germanium flat, G1, which was at a 45° angle to the laser axis. Approximately 40 % of the infrared radiation was reflected towards the monitoring equipment while the remainder of the beam passed through the flat and towards the light beam chopper. The visible red beam from a HeNe laser, H1, was introduced, via mirror M1, by reflecting it from the rear surface of the germanium flat. The alignment of this HeNe beam was adjusted so as to make it coaxial with the main CO<sub>2</sub> laser beam. After passing through the chopper wheel, C1, the main beam passed through the anti-reflection coated germanium flat G2. The small fraction of the energy reflected by G2 was directed onto a sensitive thermal image plate by mirror M4. The image on this screen could be used to visually check the output profile and intensity of the CO<sub>2</sub> laser. Another HeNe laser, H2, and turning mirror, M5, were used to mark the main CO<sub>2</sub> beam emerging from G2. This main beam was then used in the qualitative and quantitative reflectance studies which are described in sections 4.3 and 4.4.

The infrared beam reflected from G1 was sent through a zinc selenide beamsplitter B1. This beamsplitter transmitted 20 % of the energy, and this was focussed into the laser spectrum analyzer using a 30 cm focal length mirror M2.

UNCLASSIFIED

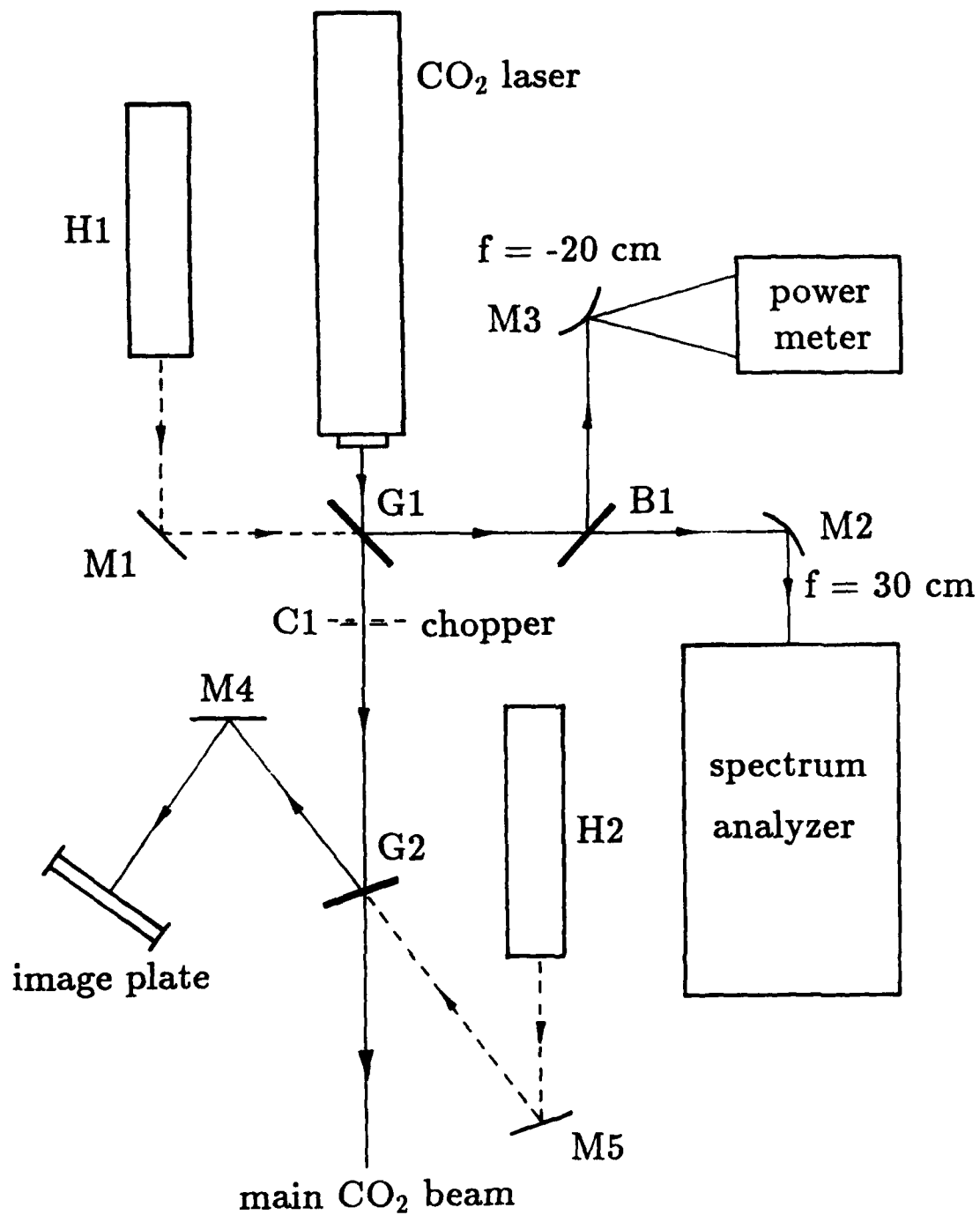


Figure 4.1: Arrangement used to obtain and monitor CO<sub>2</sub> laser beam

UNCLASSIFIED

The wavelength of the CO<sub>2</sub> laser was fixed on the 10P(20) transition for all the reflectance measurements reported here. This corresponded to a wavelength of 10.591  $\mu\text{m}$ . The 80 % of the IR beam reflected from the beamsplitter, B1, was measured by the laser power meter. A 20 cm convex mirror, M3, expanded the beam to fill the 50.8 mm diameter absorbing surface of the power meter.

## 4.2 Calibration of the HgCdTe detectors

The calibration of the photoconductive HgCdTe detectors was required for the quantitative reflectance measurements. The responsivities (volts per watt) of the detectors had to be determined so that the voltage signals due to the IR radiation reflected from the various target surfaces could be converted into units of power.

The operation of the preamplifier units, supplied for use with the HgCdTe detectors, was checked by measuring the voltage gain of each of the two units with the aid of a function generator and a resistor-dividing network. The latter was used to ensure that the input impedance to the preamplifier matched that of the detector when it was operating at 77 K. At a frequency of 500 Hz the preamplifier which was matched to the 1 mm<sup>2</sup> detector had a gain of 40 dB while that of the 4.1 mm<sup>2</sup> detector was found to be 60 dB.

The responsivities of the detector/preamplifier units were determined by putting a known amount of CO<sub>2</sub> laser radiation on each of the HgCdTe detectors. Polyethylene sheets were used to attenuate an expanded, apertured-down CO<sub>2</sub> laser beam which had previously been measured using the Scientech power meter. The 4.1 mm<sup>2</sup> detector/preamplifier combination was found to have a responsivity of 1156 V/W while that of the 1 mm<sup>2</sup> unit was 370 V/W. Both detectors were operated with a supply voltage of 10 V and a bias current of 30 mA.

## 4.3 Reflectance Study using the Infrared Camera

The main CO<sub>2</sub> laser beam, as obtained previously by the arrangement of Figure 4.1, was expanded using the folded mirror path shown in Figure 4.2. In this qualitative reflectance study the IR radiation did not have to be chopped and so the chopper wheel was removed from the beam. Mirrors M6, M7, and M9 were flat, with M9 having a diameter of 102.6 mm. Mirror M8 was convex with a focal length of  $f = -10$  cm, and M10 was a 300 cm focal-length, 102.6 mm diameter concave mirror. The variable aperture, I1, limited the final beam size at the target surface. The beam diameter at the target was of the order of 18 cm and the nominal laser intensity was approximately 4 mW/cm<sup>2</sup>.

UNCLASSIFIED

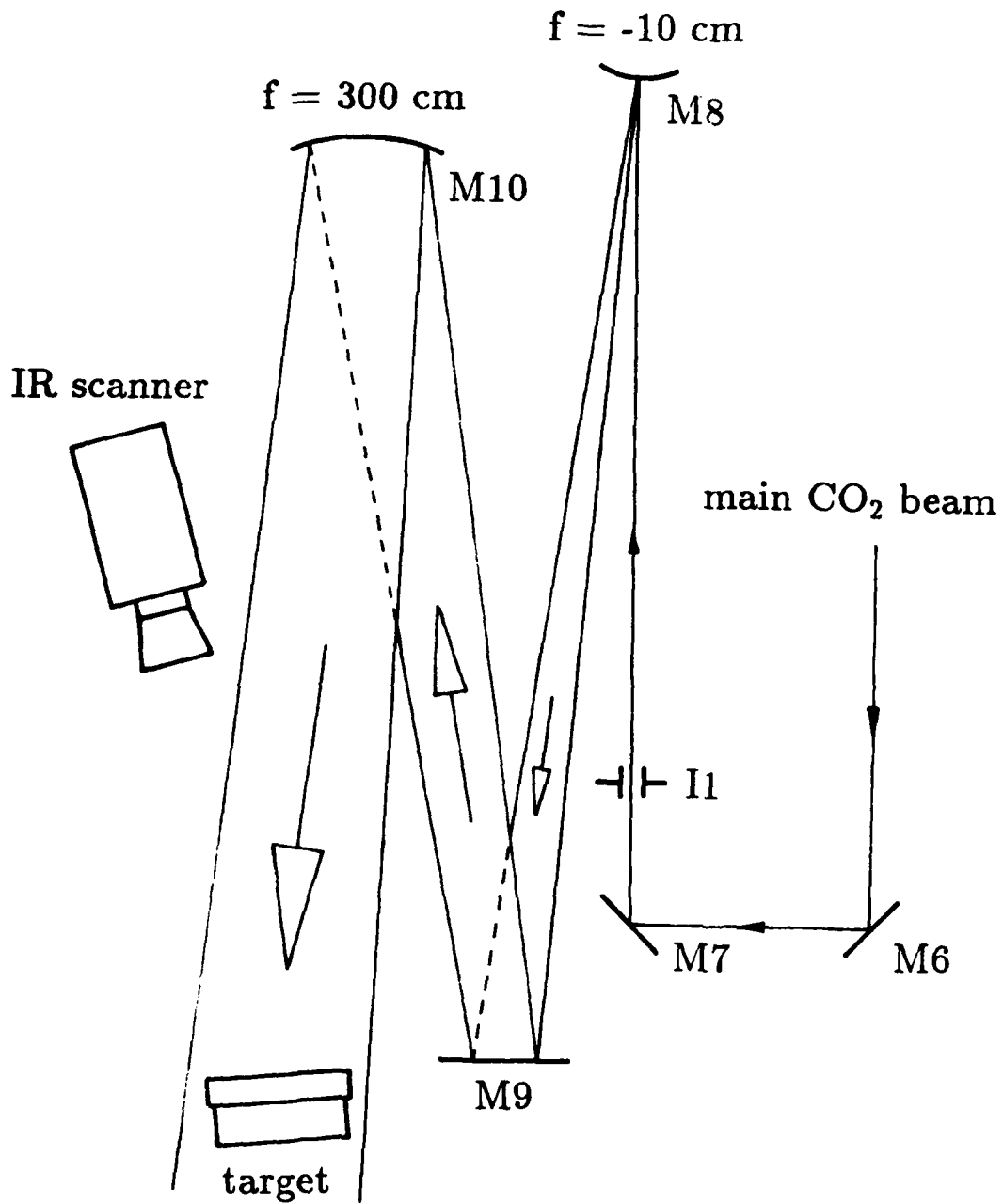


Figure 4.2: Arrangement for qualitative study of reflectance

UNCLASSIFIED

When the 20° FOV lens was being used the IR scanner was mounted on the optical table itself, while with the 3.5° lens the infrared camera was mounted on a tripod adjacent to the table. The angle of the target was adjusted so that the reflected IR radiation was directed towards the IR scanner. The gain and offset settings of the IR camera system were varied to obtain a suitable image of the target prior to digitization. Note that unlike the quantitative measurements, where retro-reflectance was considered, this qualitative study was looking at the specular reflectance from the various targets.

#### 4.4 Quantitative Reflectance Measurements

The measurements to obtain numerical reflectance data at 10.6  $\mu\text{m}$  used the configuration shown in Figure 4.3. The angles of illumination and detection were always equal and the reflectance data correspond to the case of retroreflection from the target surface.

The chopped main beam from the CO<sub>2</sub> laser was split by the zinc selenide beamsplitter B2. This had a 27/73 reflectance-to-transmittance ratio for the 45° angle at which it was used. The chopper was operated with a 10-slot blade at a rotational speed which resulted in a chopping frequency of 500 Hz. The portion of the main CO<sub>2</sub> beam transmitted by the beamsplitter was expanded with a convex mirror M9 and absorbed by an angled surface. It would have been desirable to use this transmitted beam to monitor the laser profile during measurements, but the signals reflected by the thermal image plate screens were comparable to those from some of the diffuse targets and thus interfered with the reflectance measurements.

The infrared beam reflected from B2 was incident on the target which was mounted vertically on a stage which could be rotated about a vertical axis. This platform enabled the target aspect angle,  $\theta$ , to be measured to an accuracy of  $\pm 0.25$  degrees. The replica mines were mounted such that a flat portion of the mine served as the target surface. Figure 4.4 shows the particular target areas on each of the replica mines used in the quantitative 10.6  $\mu\text{m}$  reflectance measurements. These areas were as follows;

- TMN-46: flat region on the bottom,
- PMN-6: center of rubber top cover,
- OZM-3: center of end surface,
- PFM-1: flat portion of "wing".

UNCLASSIFIED

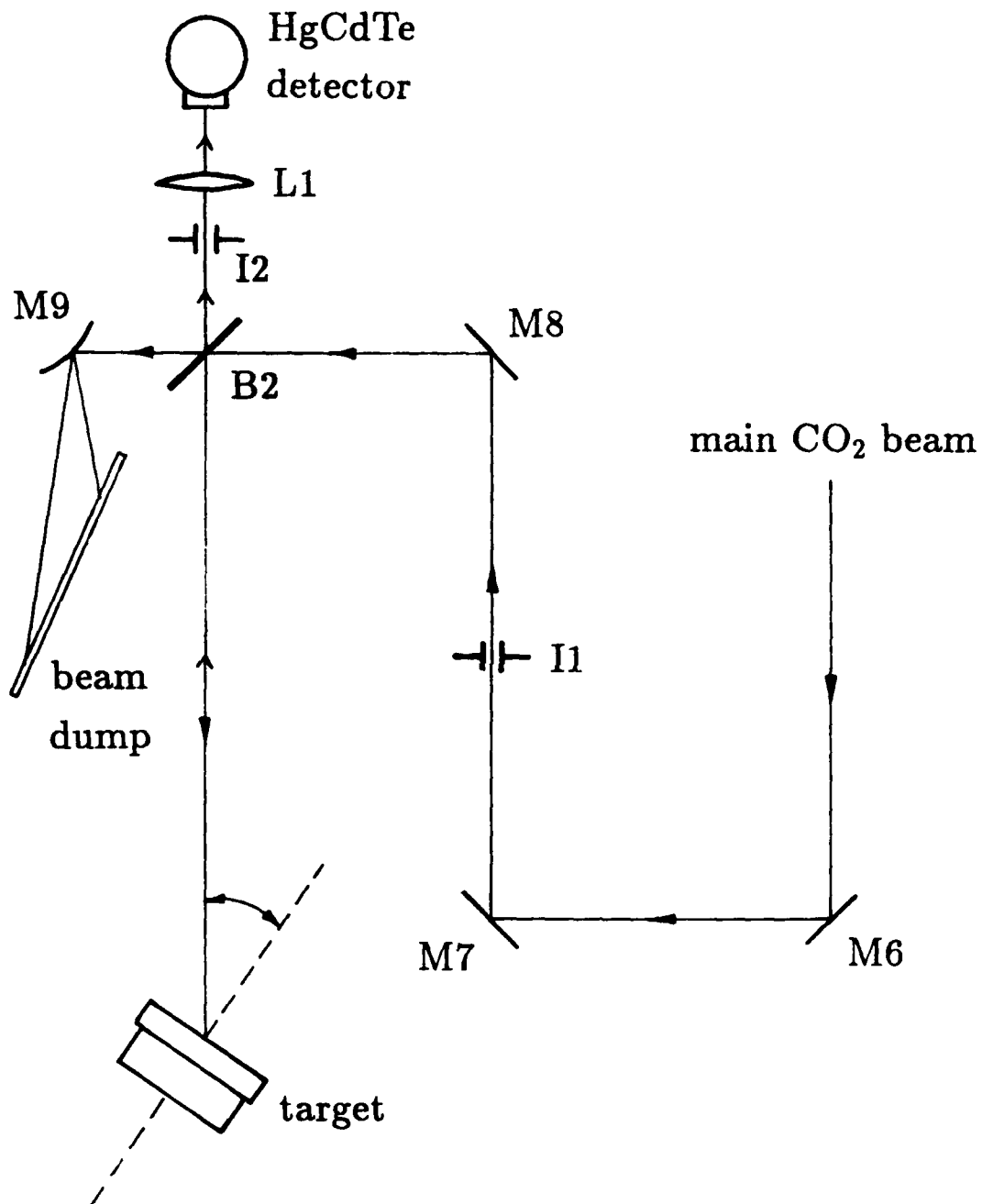
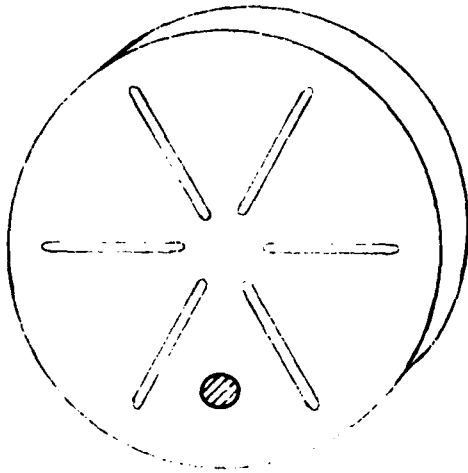


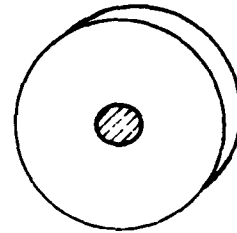
Figure 4.3: Arrangement for quantitative reflectance measurements

UNCLASSIFIED

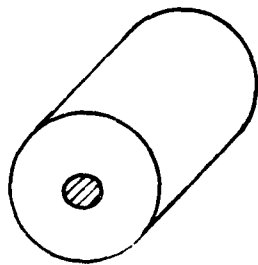
UNCLASSIFIED



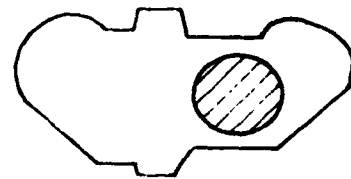
TMN-46



PMN-6



OZM-3



PFM-1

Figure 4.4: Target areas on replica mines

UNCLASSIFIED

The position at which  $\theta = 0^\circ$  was determined by finding the position where the reflected signal power was a maximum. An adjustable iris, I1, was used to control the size of the infrared beam at the target. With the iris I1 fully open the average power of the incident infrared radiation at the target surface was 0.5 W. The elliptical spot on the target had an area of approximately  $2.3 \text{ cm}^2$ , which corresponded to a laser intensity of  $0.22 \text{ W/cm}^2$ . The total distance between the output coupler of the  $\text{CO}_2$  laser and the target surface was 340 cm.

The reflected radiation from the target returned through the beamsplitter B2, with 73 % passing through to the detection optics. This infrared signal was collected and focused onto a HgCdTe detector by a  $f \approx 10 \text{ cm}$  zinc selenide lens, L1, which was 100 cm from the target surface. An iris, I2, was located just in front of the lens and was used to limit the aperture of the detection system. For specular targets I2 had a diameter of 2 cm, the area of the aperture was  $\pi \text{ cm}^2$ , and the solid angle subtended at the target was  $\pi(10^{-4})$  steradian. The majority of the reflectance measurements were made with the  $4.1 \text{ mm}^2$  HgCdTe detector and the detector with the smaller active area was used only with some of the highly-specular targets. For the measurements of the diffuse targets the aperture was  $3.2\pi \text{ cm}^2$  and the detector field of view was  $4(10^{-4}) \text{ sr}$ . The collecting lens was used for speckle averaging and had the added benefit of increasing the signal levels of the HgCdTe detector.

## 5. Results

### 5.1 Qualitative Studies

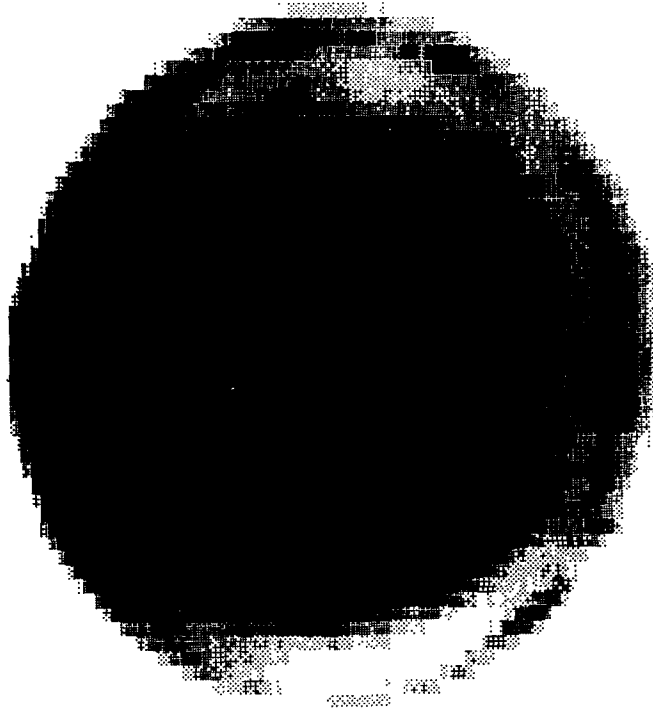
The information from the experiments with the infrared camera system proved to be very useful. A material could be readily classified as to whether its reflectance was predominantly specular or diffuse. For more complicated objects, such as the replica mines, the specific parts of the mines which were specular in the infrared were quickly identified, and shape effects were characterized. The camera was limited by thermal blooming (detector saturation) but this effect could be negated by judicious choice of the incident and camera angles.

Figure 5.1 shows the image of the replica PMN-6 mine illuminated with 10.6  $\mu\text{m}$  infrared radiation and Figure 5.2 shows that of the PFM-1 replica mine. Both images were obtained using the 20° lens, the 10.6  $\mu\text{m}$  filter, and by digitizing the frame using the arrangement described in Section 3.3. In these images the areas of the most intense IR reflection are the darkest. The strong reflection seen at the bottom of the PFM-1 image is due to a 12 mm diameter aluminum post used to support the mine. Note that some of the finer detail, visible when the images are displayed on the computer screen, has been lost in the printing and reproduction process.

The infrared reflectances of the PMN-6, OZM-3, and TMN-46 replica mines were all very specular. The PFM-1 replica mine was also somewhat specular but far less so than any of the other three mine types. This mine was the only one to have a significant diffuse component. Both the "rough" flame-sprayed aluminum and the canvas were diffuse, with the FSA having a stronger reflectance than the canvas. The "smooth" FSA was very specular.

UNCLASSIFIED

SM 1264



**Figure 5.1**  
**ACTIVE INFRARED IMAGE OF REPLICA PMN-6 MINE**

UNCLASSIFIED

## 5.2 Quantitative Reflectance Data

The output voltage of the HgCdTe detector used to measure the target reflectivity was converted into a signal power,  $P_d$ , through the use of the measured detector responsivity. For the specular targets, namely the replica mines and the "smooth" flame-sprayed aluminium plate, the reflectivity was calculated as

$$R_{spec}(\theta) = \frac{P_d}{P_{spec}}$$

where  $P_{spec}$  is the power which would have been detected from a perfectly-reflecting mirror at normal incidence. The effective Lambertian reflectivities  $R_{diff}(\theta)$  of the diffuse targets, namely the "rough" FSA plate and the canvas, were determined using the results of Section 2.2. The Fresnel number of the collection system was  $N_F \approx 34$  which resulted in very effective speckle averaging. Approximately  $[2N_F^2] \approx 2300$  speckle cells were within the aperture of the detection system used with the diffuse targets.

### 5.2.1 Replica Mines

The 10.6  $\mu\text{m}$  reflectances of the TMN-46, PMN-6, and OZM-3 replica mines were characteristically specular with high peak values at normal incidence and sharp angular dependences. Figure 5.3 gives the measured reflectance curve for the TMN-46 replica mine while Figure 5.4 shows the results for the PMN-6 and OZM-3 replica mines.

The TMN-46 mine had the strongest peak retro-reflection and its reflectance distribution had a half-width at half maximum (HWHM) of 2.2°. The PMN-6 had the sharpest drop-off, with a HWHM of 0.5°, while the replica OZM-3 mine had a HWHM of 1.7°. The replica PFM-1 mine (Figure 5.5) also had a predominantly specular reflectance but the peak value was two orders of magnitude less than that of the replica TMN-46 mine. The peak reflectance of the TMN-46 mine was 18 % while that of the PFM-1 mine was only 0.17 %. The PFM-1 reflectance curve had a HWHM of 5° and this was broader than that of any of the other replica mines.

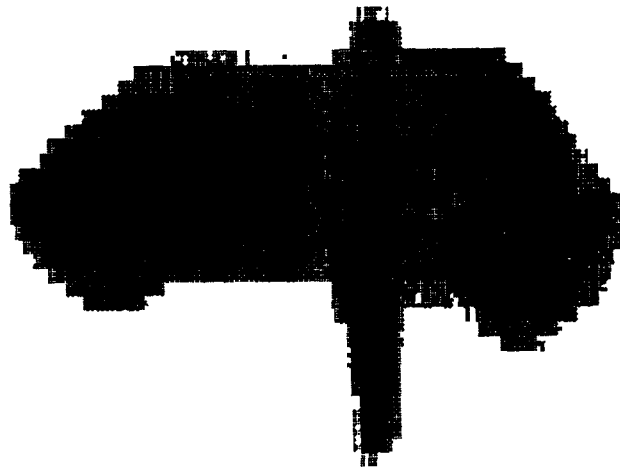


**Figure 5.2**  
**ACTIVE INFRARED IMAGE OF REPLICA PFM-1 MINE**

UNCLASSIFIED

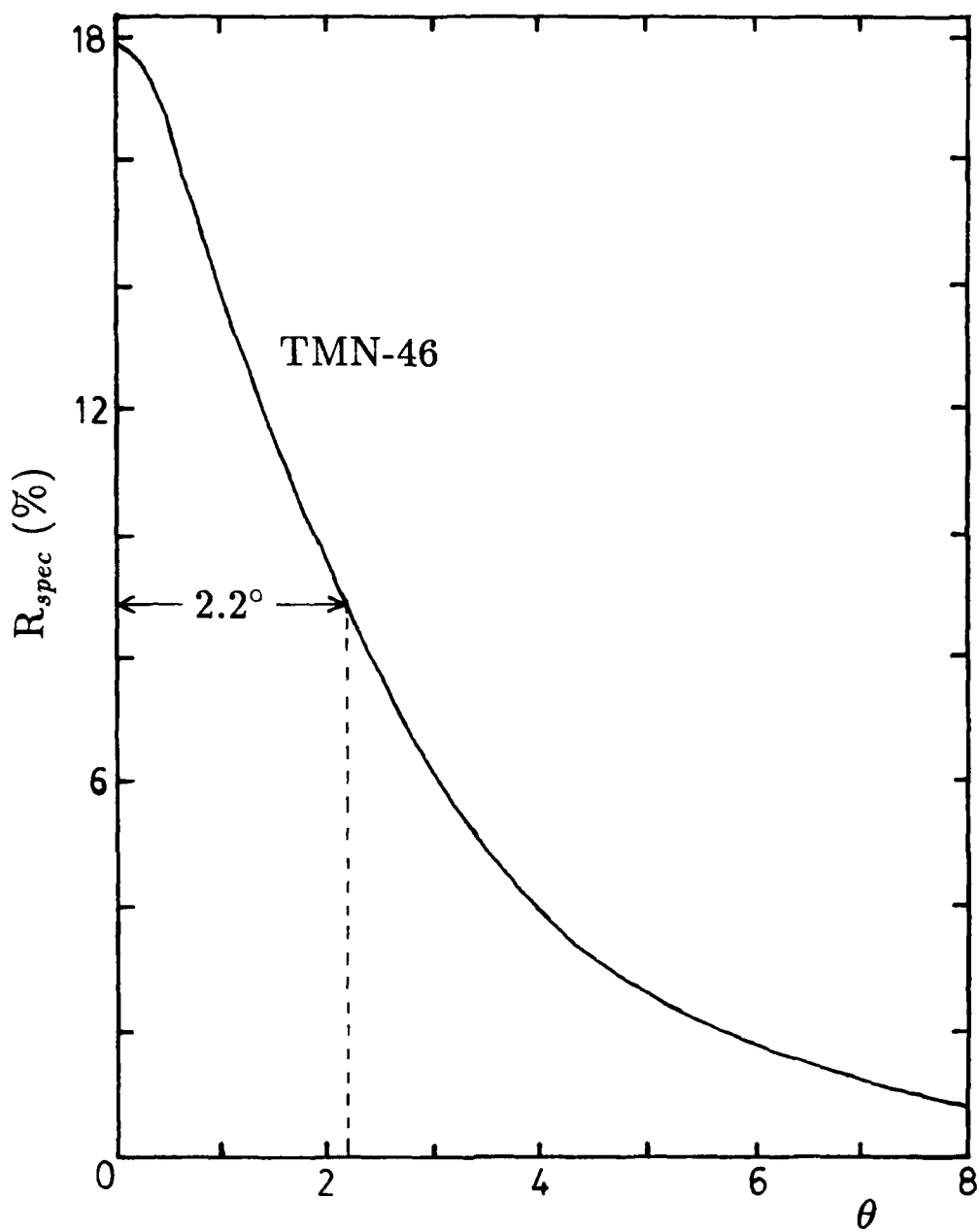


Figure 5.3: Reflectance curve for replica TMN-46 mine

UNCLASSIFIED

UNCLASSIFIED

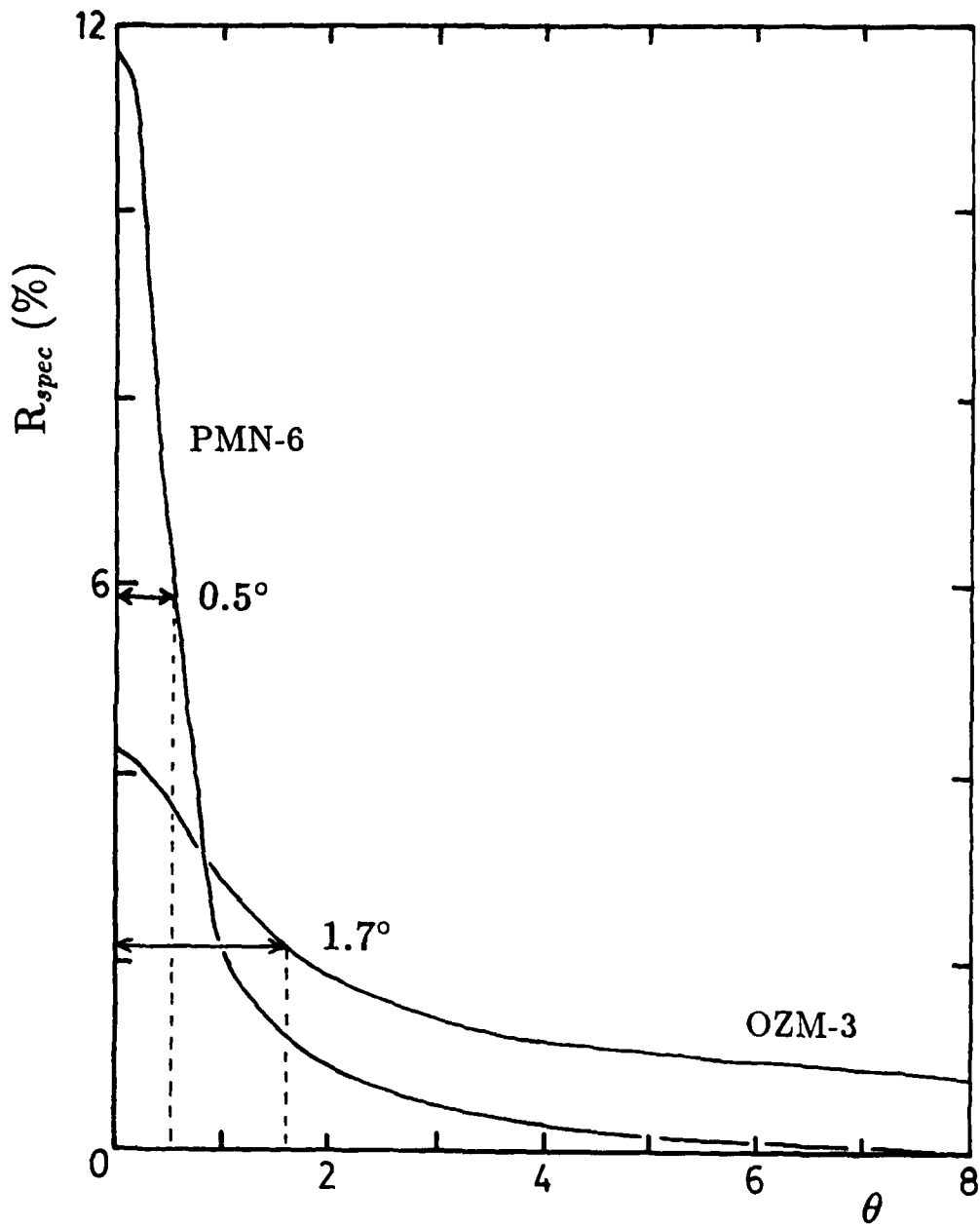


Figure 5.4: Reflectance curves for replica PMN-6 and OZM-3 mines

UNCLASSIFIED

UNCLASSIFIED

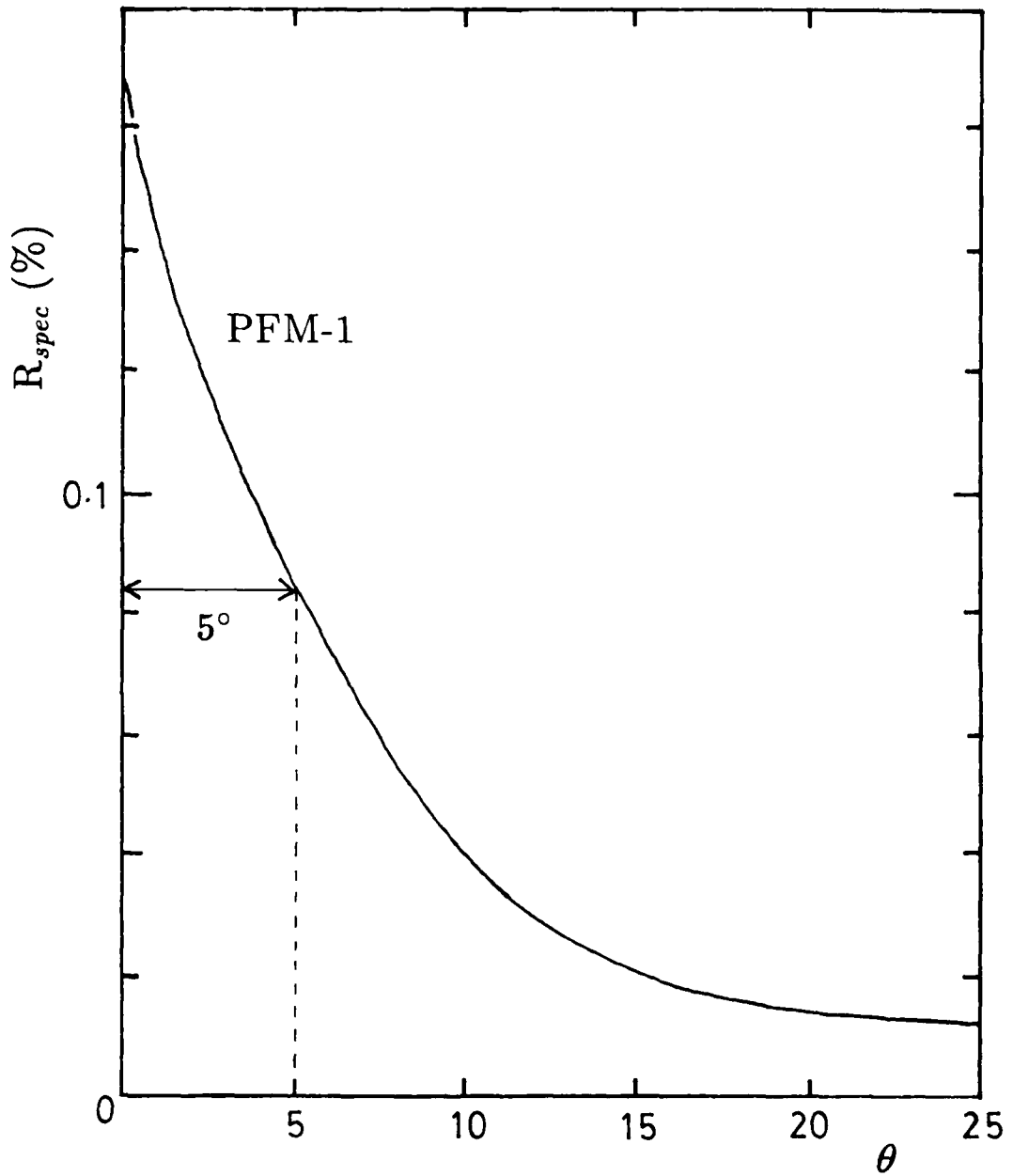


Figure 5.5: Reflectance curve for replica PFM-1 mine

UNCLASSIFIED

### 5.2.2 Reference Targets

The "smooth" flame-sprayed aluminum plate had a large specular peak (Figure 5.6) while the "rough" FSA sample had a much flatter reflectance curve (Figure 5.7). The canvas target had a reflectance similar to that of the "rough" flame-sprayed aluminum plate but with a smaller peak value. The peak diffuse reflectivities,  $R_{diff}(0)$ , of the "rough" FSA and the canvas were 2.0 and 0.3 respectively.

UNCLASSIFIED

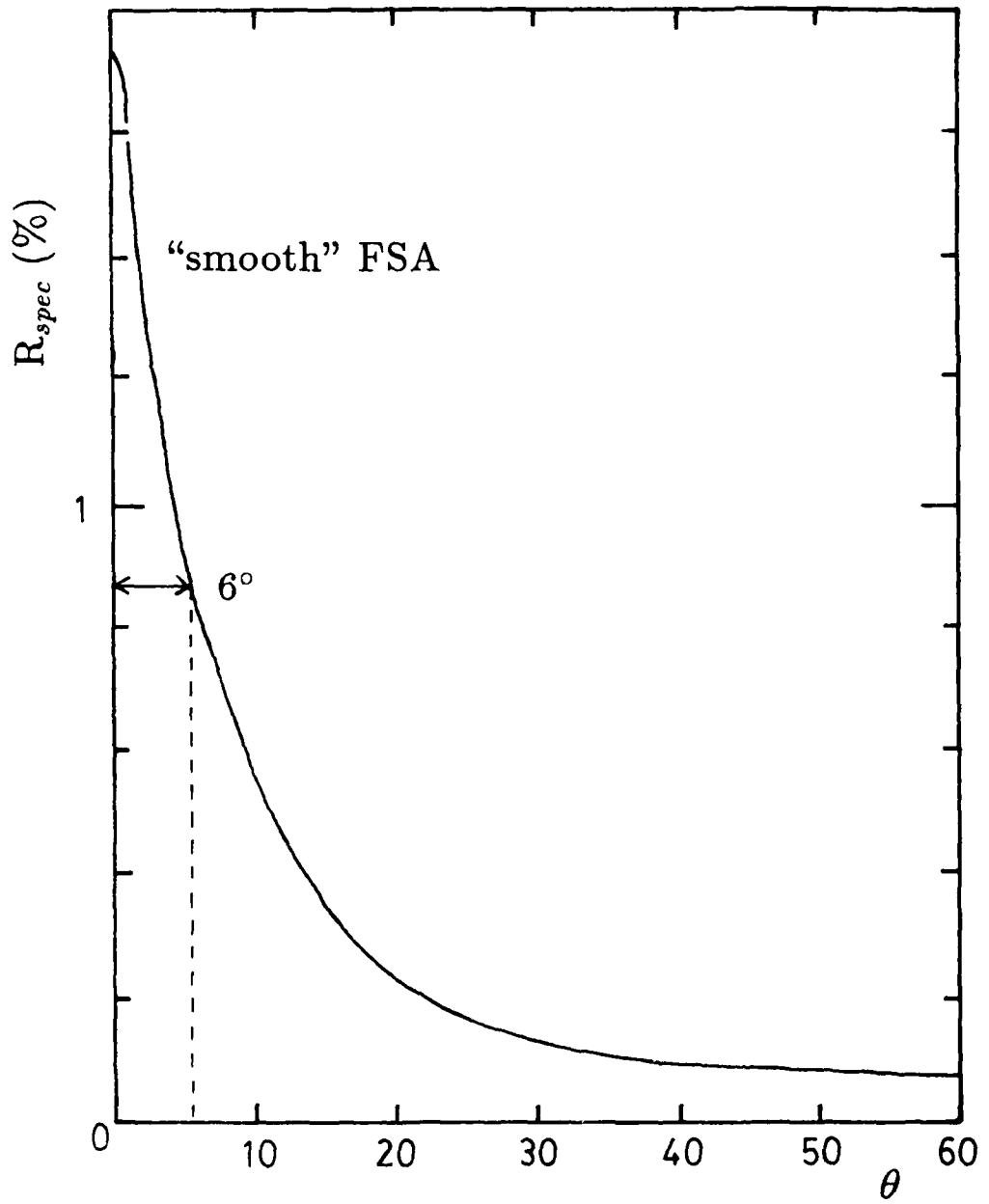


Figure 5.6: Reflectance curve for "smooth" FSA plate

UNCLASSIFIED

UNCLASSIFIED

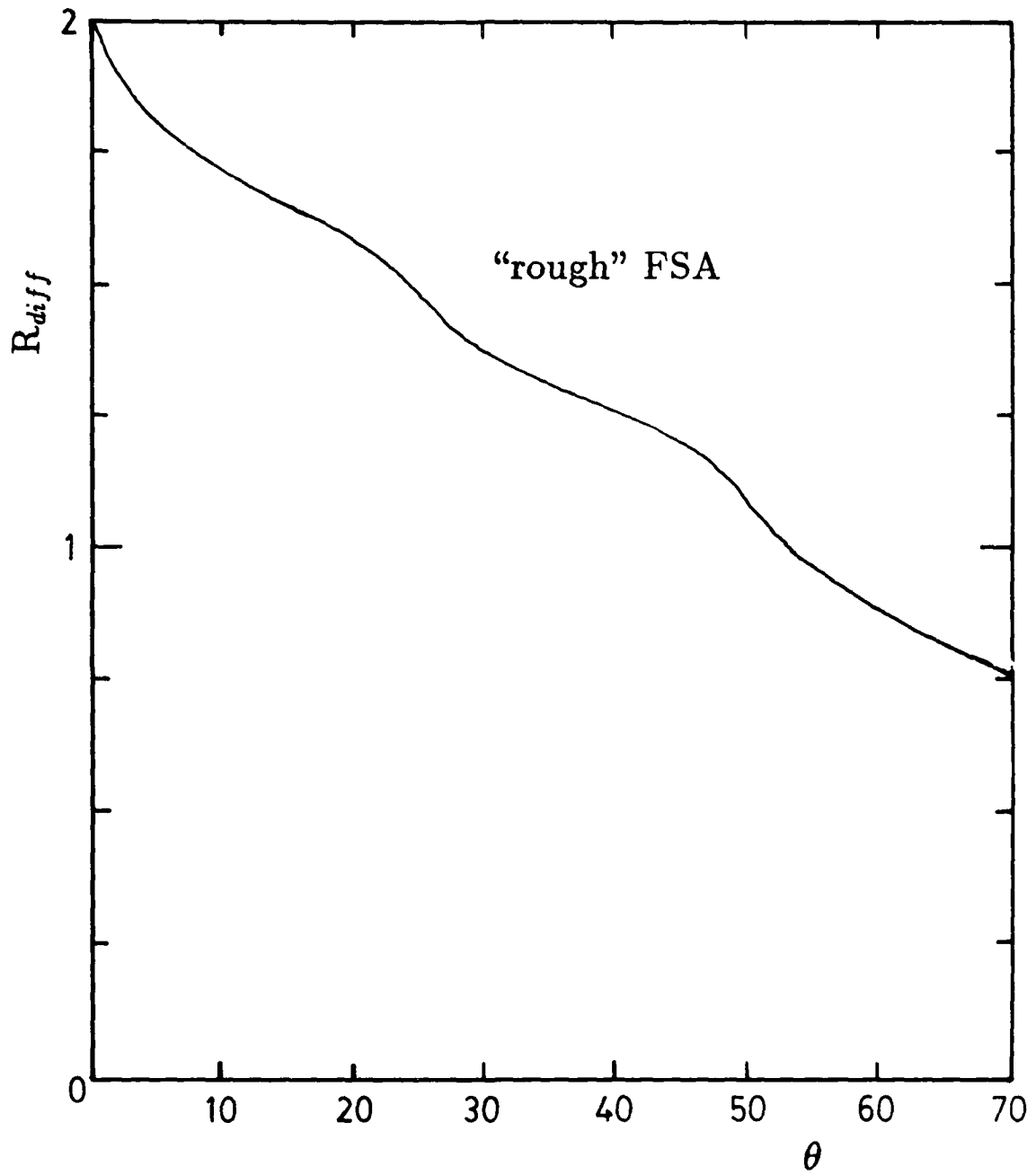


Figure 5.7: Reflectance curve for "rough" FSA plate

UNCLASSIFIED

UNCLASSIFIED

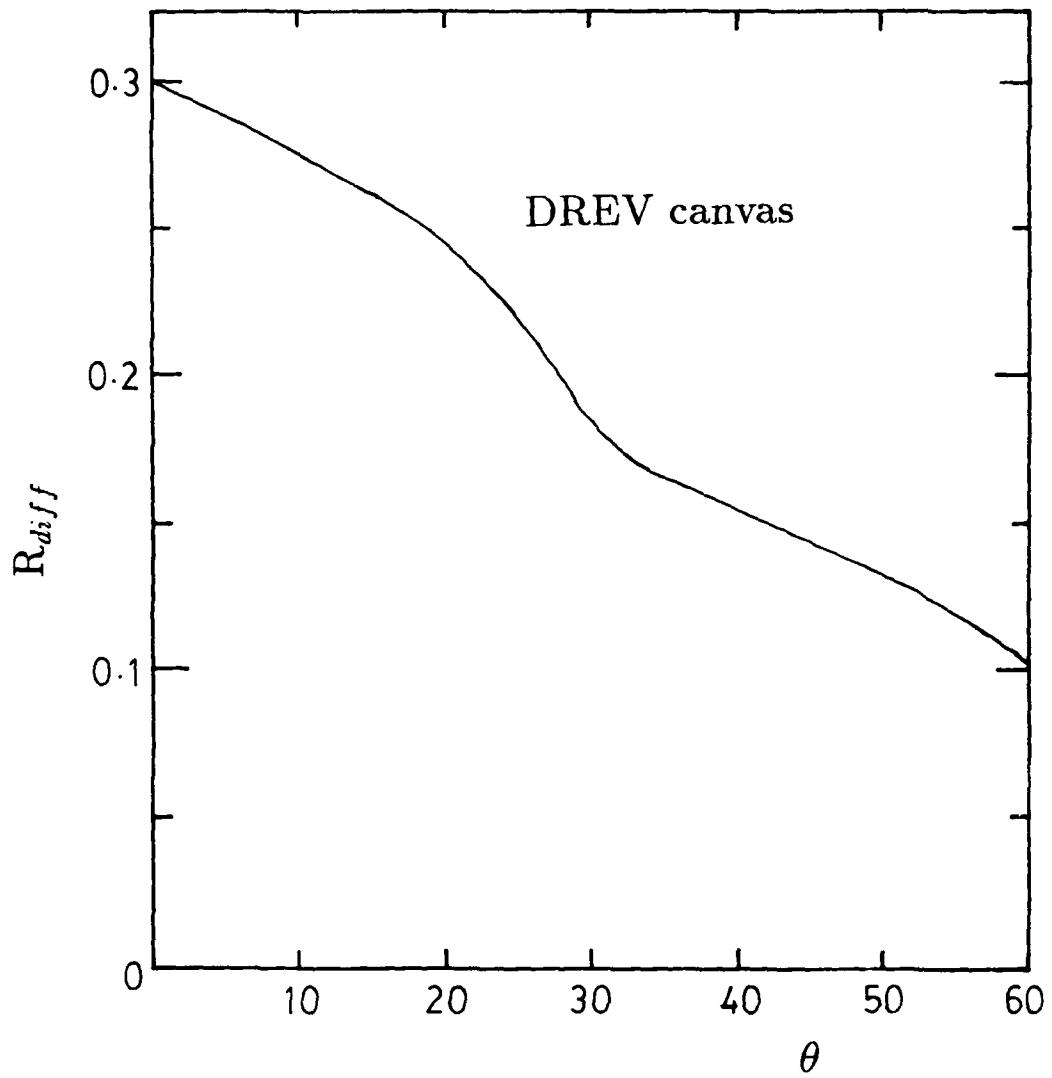


Figure 5.8: Reflectance curve for canvas

UNCLASSIFIED

## 6. Discussion

### 6.1 Summary of Results

All of the replica mines were found to have 10.6  $\mu\text{m}$  reflectivities which were characteristic of predominantly specular targets. Three of the replica mines had substantial specular reflectances;  $R_{\text{spec}}(0) = 18\%$ ,  $12\%$ ,  $4\%$  for the TMN-46, PMN-6, and OZM-3 mines respectively. The reflectance of the replica "butterfly" mine was, however, only  $0.2\%$ . The specular peaks for all of the mines had half-width, half-maximums of  $\text{HWHM} \leq 5^\circ$ .

Both the "rough" flame-sprayed aluminum and the canvas were found to have reflectances which corresponded fairly well to those measured by other researchers. The  $\theta = 0^\circ$  retro-reflectance of the "rough" FSA was found to be  $R_{\text{diff}}(0) = 2.0$  which is within the typical range of reflectances for flame-sprayed and sand-blasted aluminum samples [6] [7].

The retro-reflection at  $0^\circ$  for the canvas was nearly twice as large as that reported by [6], where spinning targets were used for speckle-averaging. However the ratio of the reflectivity at  $0^\circ$  to that at  $30^\circ$  was found to be 1.7 which was very close to the previously measured ratio of 1.6. The lower effective Lambertian reflectivities for the spinning canvas target could be due to the fact that the canvas is a woven material. When the fibers are oriented exactly perpendicular and parallel to the direction of polarization of the incident  $\text{CO}_2$  laser radiation, as was the case here, one might expect the reflection to be greater than when the fibers are at other angles.

Using an IR camera system and  $\text{CO}_2$  laser illumination the qualitative characteristics of reflectance for the replica mines were quickly determined. Differences due to materials and shape effects were apparent.

### 6.2 Specular Mines and RMD

These preliminary measurements using the replica mines confirm that remote minefield detection is, in its broadest terms, a problem of locating specular targets in a more diffuse background. The results support the need to locate the RMD

system on an airborne platform which will enable the imaging CO<sub>2</sub> laser radar to look downwards and have the greatest possibility of detecting the strong returns from the scatterable mines. The specularity of mines also suggests that the field-of-view of the airborne RMD sensor will be no greater than 10°. This is also probably the limit due to the requirement for high resolution scanning which must yield pixels of a few cm on the ground from heights of 100 m or more. A 10° FOV RMD system is therefore indicated by both the target reflectance characteristics and by the data acquisition capability.

The relatively small reflectance of the replica PFM-1 scatterable mine demonstrates that there are some mine materials which would be difficult to detect with an active thermal IR system. Different materials, coatings, and shapes can all be used as RMD countermeasures and must be investigated.

### **6.3 Future Studies**

Future reflectance measurements on mines and mine-like objects should focus on determining the IR retroreflection at aspect angles less than 10°. Ideally the experimental geometry should as closely as possible duplicate that of an actual RMD laser radar in terms of the spot size of the laser beam, detector field-of-view etc. To achieve the necessary target distances these experiments may have to be conducted in the field. Additional mine data will be useful in the simulation of active IR images which will be used to investigate image processing techniques.

These preliminary experiments did not consider the polarization of the reflected 10.6 μm radiation but future studies must consider polarization effects. Monostatic laser radars use polarization switches to separate the transmitted and received signals so the polarization state of the return from the target is important. In addition a heterodyne-detection system is polarization-dependent while for a direct-detection system only the magnitude of the signal affects the detection process itself. A grid polarizer and lock-in amplifier have been obtained for use in future experiments where polarization effects will be studied.

Further study of convenient CO<sub>2</sub> reference targets should be undertaken. Most of the published data for such targets gives the angular distribution of the reflected IR radiation for a given angle of incidence. Determining this angular distribution rather than only the retro-reflected signal will allow for better comparison to previously published results. Other lightweight, flexible targets similar to the canvas should be investigated. Such targets have been developed [8] and found to have nearly constant reflectances over incidence angles of up to ± 60°. The dependence on the orientation of the canvas sample should be studied to quantify any effects due to the direction of the fibers within the sample. The canvas target can be mounted in a spinning holder

as done by [6].

The IR camera system can be used to give a rapid qualitative assessment of target reflectivity, and is particularly useful in the study of shape effects. With the 3.5° lens it can be used in experiments in the field which closely duplicate the geometry of the RMD system. The potential to obtain active IR images of scaled minefields also exists.

In summary, future studies should provide

- retro-reflective data ( $\theta < 10^\circ$ ) on mines, mine-materials, and mine-coatings,
- angular distribution of reflectance from reference targets such as canvas,
- polarization information on the reflected IR radiation,
- and quantitative reflectance information using IR camera system.

## 7. References

- [1] G. C. Stuart. *Remote minefield detection using infrared laser radar (U)*. Suffield Memorandum 1223, Defence Research Establishment Suffield, 1988 UNCLASSIFIED.
- [2] J. E. McFee, K. Russell, M. Ito, G. C. Stuart, and Y. Das. A hierarchical scheme for analysis of minefield images (U). In *Proceedings of DREV Signal-Processing Conference*, 1988 UNCLASSIFIED.
- [3] MILTRA. *Military Training Product Information*. Division of Z. M. Iwaszko Limited, 357 Uxbridge Road, Rickmansworth, Herfordshire England, 1988.
- [4] R. A. Brandewie and W. C. Davis. Parametric study of a 10.6 micron laser radar. *Applied Optics*, 11(7):1526, 1972.
- [5] M. J. Kavaya, R. T. Menzies, and D. A. Haner et. al. Target reflectance measurements for calibration of lidar atmospheric backscatter data. *Applied Optics*, 22(17):2619, 1983.
- [6] H. Henshall and J. Cruickshank. Reflectance characteristics of selected materials for reference targets for 10.6  $\mu\text{m}$  laser radars. *Applied Optics*, 27(13):2748, 1988.
- [7] J. E. Eberhardt, J. G. Haub, and A. W. Pryor. Reflectivity of natural and powdered minerals at CO<sub>2</sub> laser wavelengths. *Applied Optics*, 24(3):388, 1985.
- [8] T. K. Lea and R. M. Schotland. Infrared retroreflecting lidar calibration target. *Applied Optics*, 27(2):208, 1988.

# **Appendix A**

## **Equipment Information**

device	manufacturer	model
CO <sub>2</sub> laser CO <sub>2</sub> laser power supply HeNe lasers  optical table top vibration-isolation system	MPB Technologies Glassman Melles Griot Spectra Physics TMC TMC	GN-802-GES LP-20P-6M4A 05-LLP-805 115 Micro-g 76-458-1 Micro-g 62-125
laser spectrum analyzer thermal plates HgCdTe detectors laser power meter digital indicator	Optical Engineering Optical Engineering Infrared Associates Scientech Scientech	16A  HCT-80, HCT-100 36-0201 36-0365
light beam chopper oscilloscopes	Ithaco Tektronix	230 7834, 466
dc power supply digital multimeter function generator	Anatek Fluke Hewlett Packard	6020 8000A 811A
infrared camera scan converter video monitor video digitizer personal computer laser printer	AGA (Agema) Viewscan Sony Newtek Commodore Hewlett Packard	Thermovision 782 LWB 700 Trinitron CVM-1270 Digi-View Amiga LaserJet Series II

Table A.1: List of equipment used in IR reflectance studies

<b>DOCUMENT CONTROL DATA - R &amp; D</b>		
<small>(Security classification of title, body of abstract and indexing annotation must be entered when the overall document is classified)</small>		
<b>1 ORIGINATING ACTIVITY</b>  Defence Research Establishment Suffield	<b>2a. DOCUMENT SECURITY CLASSIFICATION</b> Unclassified	
	<b>2b. GROUP</b>	
<b>3 DOCUMENT TITLE</b>  Infrared Reflectance Measurements of Replica Mines and Reference Targets (U)		
<b>4 DESCRIPTIVE NOTES (Type of report and inclusive dates)</b>  Suffield Memorandum		
<b>5 AUTHOR(S) (Last name, first name, middle initial)</b>  STUART, Gregory C.		
<b>6 DOCUMENT DATE</b> February 1989	<b>7a. TOTAL NO. OF PAGES</b> 39	<b>7b. NO. OF REFS</b> 8
<b>8a. PROJECT OR GRANT NO.</b>  031SD	<b>9a. ORIGINATOR'S DOCUMENT NUMBER(S)</b>  SM 1264	
<b>8b. CONTRACT NO.</b>	<b>9b. OTHER DOCUMENT NO.(S) (Any other numbers that may be assigned this document)</b>	
<b>10. DISTRIBUTION STATEMENT</b>  Unlimited		
<b>11 SUPPLEMENTARY NOTES</b>	<b>12. SPONSORING ACTIVITY</b>	
<b>13. ABSTRACT</b>  <p>The 10.6 <math>\mu\text{m}</math> reflectance characteristics of a number of targets were measured to establish a preliminary database for studies in remote minefield detection (RMD) and to verify experimental techniques. The reflectivities of typical mine-casing materials and mine paints were found to be highly specular, although there was substantial variation in the magnitudes of the returns. The measured reflectances of diffuse reference targets were in reasonably good agreement with previously published data.</p> <p>In addition to the numerical results, a qualitative study of reflectance using an infrared camera and <math>\text{CO}_2</math> laser illumination proved useful in the rapid investigation of target reflectivity. The implications of the results of the study of mine materials to the feasibility of airborne RMD are discussed and suggestions are made for future in-depth experiments.</p>		

## KEY WORDS

reflectance  
infrared  
CO<sub>2</sub> lasers  
10.6 microns

## INSTRUCTIONS

1. **ORIGINATING ACTIVITY** Enter the name and address of the organization issuing the document.
- 2a. **DOCUMENT SECURITY CLASSIFICATION** Enter the overall security classification of the document including special warning terms whenever applicable.
- 2b. **GROUP** Enter security reclassification group number. The three groups are defined in Appendix 'M' of the DRB Security Regulations.
3. **DOCUMENT TITLE** Enter the complete document title in all capital letters. Titles in all cases should be unclassified. If a sufficiently descriptive title cannot be selected without classification, show title classification with the usual one-capital-letter abbreviation in parentheses immediately following the title.
4. **DESCRIPTIVE NOTES** Enter the category of document, e.g. technical report, technical note or technical letter. If appropriate, enter the type of document, e.g. interim, progress, summary, annual or final. Give the inclusive dates when a specific reporting period is covered.
5. **AUTHOR(S)** Enter the name(s) of author(s) as shown on or in the document. Enter last name, first name, middle initial. If military, show rank. The name of the principal author is an absolute minimum requirement.
6. **DOCUMENT DATE** Enter the date (month, year) of Establishment approval for publication of the document.
- 7a. **TOTAL NUMBER OF PAGES** The total page count should follow normal pagination procedures, i.e., enter the number of pages containing information.
- 7b. **NUMBER OF REFERENCES** Enter the total number of references cited in the document.
- 8a. **PROJECT OR GRANT NUMBER** If appropriate, enter the applicable research and development project or grant number under which the document was written.
- 8b. **CONTRACT NUMBER** If appropriate, enter the applicable number under which the document was written.
- 9a. **ORIGINATOR'S DOCUMENT NUMBER(S)** Enter the official document number by which the document will be identified and controlled by the originating activity. This number must be unique to this document.
- 9b. **OTHER DOCUMENT NUMBER(S)** If the document has been assigned any other document numbers (either by the originator or by the sponsor), also enter this number(s).
10. **DISTRIBUTION STATEMENT** Enter any limitations on further dissemination of the document, other than those imposed by security classification, using standard statements such as:
- (1) "Qualified requesters may obtain copies of this document from their defence documentation center."
  - (2) "Announcement and dissemination of this document is not authorized without prior approval from originating activity."
11. **SUPPLEMENTARY NOTES** Use for additional explanatory notes.
12. **SPONSORING ACTIVITY** Enter the name of the departmental project office or laboratory sponsoring the research and development. Include address.
13. **ABSTRACT** Enter an abstract giving a brief and factual summary of the document, even though it may also appear elsewhere in the body of the document itself. It is highly desirable that the abstract of classified documents be unclassified. Each paragraph of the abstract shall end with an indication of the security classification of the information in the paragraph (unless the document itself is unclassified) represented as (TS), (S), (C), (R), or (U).  
  
The length of the abstract should be limited to 20 single-spaced standard typewritten lines, 7 1/4 inches long.
14. **KEY WORDS** Key words are technically meaningful terms or short phrases that characterize a document and could be helpful in cataloging the document. Key words should be selected so that no security classification is required. Identifiers, such as equipment model designation, trade name, military project code name, geographic location, may be used as key words but will be followed by an indication of technical context.

Copy available to DTIC does not  
permit fully legible reproduction